Proceedings of the Seventh International Conference on
Railway Technology: Research, Development and Maintenance
Edited by: J. Pombo
Civil-Comp Conferences, Volume 15, Paper 17.8
Civil-Comp Press, Edinburgh, United Kingdom, 2026
ISSN: 2753-3239, doi: 10.4203/ccc.15.17.8

Continuous Mobile Measurement System for Rail Profile Based on Multi-Line Laser and Combined Navigation

Y. Shi[1,2], Q. Mao[1,3,4], H. Xu[1], W. Hu[3], Y. Mu[4] and G. Wang[1]

[1]School of Remote Sensing and Information Engineering, Wuhan University, China
[2]State Key Laboratory of Rail Transit Vehicle System, Southwest Jiaotong University, Chengdu, China
[3] Wuhan Hanning Rail Transit Technology Corporation Limited, China
[4]Hubei luojia laboratory, Wuhan, China

Abstract

A continuous mobile measurement and 3D reconstruction method for rail profiles based on multi-line structured light and integrated navigation is proposed. A multi-sensor fusion localization model integrating IMU, DMI, and GNSS is developed to achieve high-precision pose estimation under dynamic conditions. A unified coordinate transformation framework is established for consistent point cloud representation. An improved ICP algorithm incorporating initial pose and structural constraints is proposed for accurate multi-temporal point cloud registration and continuous reconstruction. Experimental results demonstrate that the static measurement accuracy is better than 0.10 mm, with an optimal accuracy of 0.06 mm. Under dynamic conditions at 60 km/h, the measurement deviation is maintained within 0.10 mm. The proposed method enables the transformation from discrete cross-sectional measurement to continuous spatial reconstruction, significantly improving measurement accuracy and efficiency.

Key words: rail profile, continuous measurement, line laser, multi-sensor fusion, combined navigation, point cloud reconstruction.

1. Introduction

With the rapid expansion of high-speed and urban rail transit systems, higher requirements are imposed on rail condition monitoring in terms of accuracy, efficiency, and continuity. Rail profile, as a key indicator of track condition, directly affects vehicle-track interaction and operational safety[1],[2]. Long-term service leads to wear, deformation, and fatigue damage, making high-precision and continuous rail profile measurement essential for maintenance and condition assessment [3].

Existing rail profile measurement methods can be broadly classified into contact and non-contact approaches. Contact methods, such as MiniProf, provide high accuracy but suffer from low efficiency and are limited to discrete cross-sectional measurements, making them unsuitable for long-distance continuous inspection. In contrast, non-contact methods based on structured light have attracted increasing attention due to their high efficiency and automation capability [4].

Previous studies have demonstrated the feasibility of laser scanning for rail profile acquisition. Lichti et al. [5] used laser scanning technology to measure track geometry parameters; Gonz et al. [6] proposed a railway detection method based on laser profilometer, which effectively improved the efficiency of data acquisition. While multi-sensor fusion techniques integrating inertial measurement units (IMU), odometry (DMI), and global navigation satellite systems (GNSS) have been introduced to support mobile measurement and dynamic positioning. Sheikh et al. [7] have studied multi-sensor fusion positioning methods, providing a theoretical basis for mobile measurement systems. Puente et al. [8] applied mobile laser scanning technology to railway infrastructure inspection, achieving the acquisition and analysis of track point cloud data. Ye et al. [9] also proposed a multi-sensor integrated non-contact rail detection method, which effectively improves the stability and reliability of the system in complex environments.

In terms of accuracy improvement, structured-light-based methods have achieved high precision under static conditions [10]. Sun et al. [11] proposed a dynamic measurement error correction method based on multi line structured light. Zhou et al. further combined visual processing methods to achieve automatic extraction and analysis of rail profiles [12]. Related studies have shown that rail wear and geometric irregularities can cause wheel rail coupling vibration, which in turn affects the safety and comfort of train operation [13]. However, under high-speed motion, measurement accuracy is still affected by vibration and pose variations. Meanwhile, point cloud registration methods such as ICP are widely used for profile reconstruction, but cumulative errors remain a challenge in long-distance continuous measurements [14],[15]. These limitations restrict the ability of existing methods to achieve accurate and continuous spatial representation of rail profiles in real-world conditions.

To address these challenges, this study proposes a continuous mobile measurement and 3D reconstruction method for rail profiles based on multi-line structured light and multi-sensor fusion. A vehicle-mounted system integrating laser sensors, IMU, DMI, and GNSS is developed for synchronized acquisition of rail geometry and pose information. A multi-sensor fusion localization model is established to improve pose estimation accuracy under dynamic conditions. In addition, an improved point cloud registration and stitching method is proposed to enable continuous 3D reconstruction of rail profiles. Field experiments are conducted to validate the accuracy and stability of the proposed system.

2. Mobile Rail Profile Measurement System

To achieve high-precision, continuous, and high-speed mobile measurement of rail profiles, a rail profile measurement system based on multi-sensor fusion is developed in this study. The proposed system integrates multiple sensing modalities to enable the synchronized acquisition of rail cross-sectional geometric information and the spatial pose of the measurement platform. Combined with post-processing algorithms, continuous three-dimensional reconstruction of rail profiles is achieved, thereby meeting the requirements of efficient inspection over long railway distances.

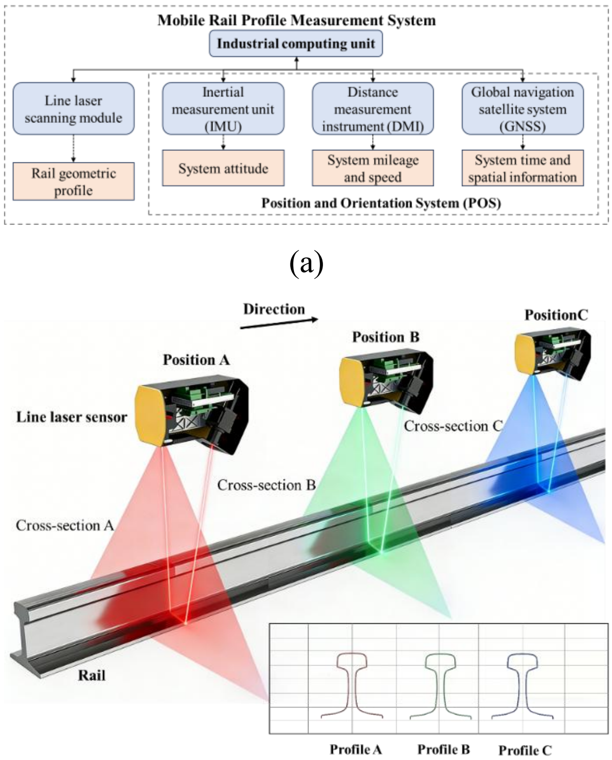

(a)

(b)

Figure 1: Mobile rail profile measurement system. (a) Schematic diagram; (b) Line laser scanning during continuous measurement.

The system adopts a modular design and consists of five core components: line laser scanning module, an IMU, DMI, GNSS, and industrial computing unit. The overall system architecture is illustrated in Figure 1(a). The line laser scanning module serves as the core component for geometric data acquisition, responsible for capturing rail profile information. The IMU, DMI, and GNSS jointly form a Position and Orientation System (POS), which provides real-time estimation of the platform's spatial position and attitude. The industrial computing unit performs multi-sensor data acquisition, time synchronization, and data processing.

During operation, all sensors are triggered based on a unified time reference to ensure temporal consistency across multi-source data. Through subsequent data fusion, discrete cross-sectional point clouds are reconstructed into a continuous 3D rail profile. The line laser scanning process during continuous motion is illustrated in Figure 1(b).

The line laser scanning module is the key component for acquiring rail geometric information. It is based on the principle of laser triangulation, in which a line-shaped laser is projected onto the rail surface and its reflection is captured by charged coupled device (CCD) camera to reconstruct the two-dimensional cross-sectional point cloud, as shown in Figure 2.

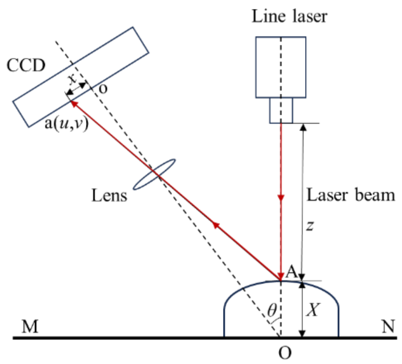

Figure 2: Schematic diagram of the laser triangulation principle.

The measurement process can be expressed as:

$$z = f(u, v, \theta, d) \quad (1)$$

where u and v denote the image pixel coordinates in 2D, θ represents the laser emission angle, d is the baseline distance determined by the laser sensor, and z corresponds to the spatial depth information. Through system calibration, the mapping relationship between image coordinates and spatial coordinates is established, enabling accurate three-dimensional reconstruction.

To achieve full cross-sectional coverage and high measurement accuracy, two high precision line structured light sensors are deployed for each rail, scanning from symmetric directions. The two laser lines overlap in the rail head region, which not only increases point cloud density but also provides redundancy for data calibration. The sensor integration and angular configuration are illustrated in Figure 3(a) and 3(b). This design effectively overcomes occlusion issues inherent in single-view measurements and improves the reliability of measurements in complex regions, such as rail head edges.

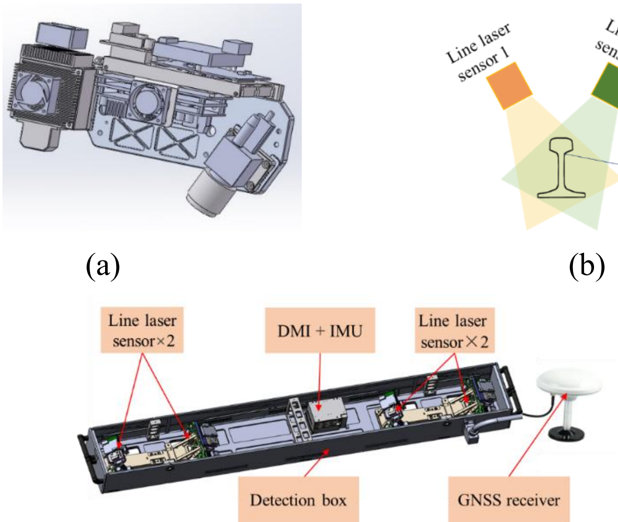

(c)

Figure 3: Measurement system. (a) Line structured light sensor module; (b) Angle of tow line laser sensors; (c) Overall system integration.

The system adopts a mounted integrated deployment scheme and can be installed on rail trolleys or vehicles, enabling rail profile measurement under different operating speeds and significantly improving inspection efficiency. The hardware configuration mainly includes mobile servers, detection box, and sensor modules. And two line laser sensors mounted at each end for detection box, with one IMU and one DMI in the middle, while the GNSS antenna is mounted externally outside the box to ensure signal quality. The internal structure of the detection beam is shown in Figure 3(c). In addition, the system follows a modular design philosophy, where each sensor integrates data acquisition, synchronization control, and communication interfaces. This design facilitates maintenance and replacement while enhancing system stability and adaptability for engineering applications.

3 Continuous Mobile Measurement Principle

To achieve high-precision continuous reconstruction of rail profiles, a unified methodological framework integrating multi-sensor fusion localization, point cloud registration and reconstruction is established, to enable the synchronized acquisition of rail cross-sectional point clouds and platform pose information through multi-sensor collaboration. By transforming and aligning multi-temporal data within a unified coordinate system, traditional discrete cross-sectional measurements are extended to continuous 3D rail profile reconstruction. The framework for continuous mobile measurement is shown in Figure 4.

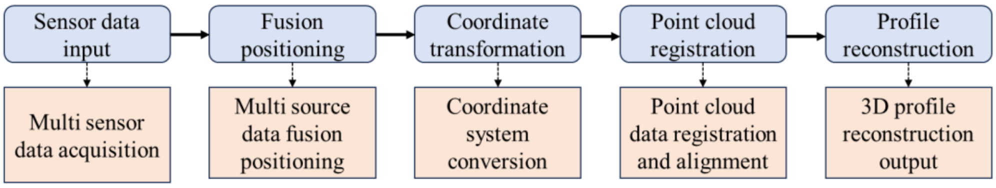

Figure 4: Methodology framework of continuous mobile measurement.

During operation, the system moves along the rail direction at a constant speed. In the process, rail cross-sectional point clouds and platform pose information are acquired simultaneously. All sensors are triggered under a unified time reference, and temporal alignment is achieved through timestamp synchronization, ensuring spatiotemporal consistency of multi-source data. At each time instant, the line laser sensor captures local cross-sectional point clouds, while the system pose is estimated by fusing IMU and DMI data. The acquired local point clouds are then transformed into the global coordinate system. As the system progresses, point clouds from successive time steps are accumulated and integrated, ultimately forming a continuous rail profile. Compared with traditional contact-based or discrete measurement methods, the proposed approach enables the transformation of rail profile measurement from “discrete cross-sections” to “continuous spatial curves.” It offers significant advantages, including non-contact measurement, high efficiency, and suitability for high-speed inspection scenarios.

3.1 Multi sensor fusion localization

In mobile measurement scenarios, the accuracy of platform pose estimation directly affects the quality of point cloud reconstruction. Single sensors are susceptible to noise and drift; therefore, a multi-sensor fusion approach integrating IMU, DMI, and GNSS is adopted [16],[17]. An Extended Kalman Filter (EKF) is employed to achieve high-precision pose estimation.

The system state vector is defined as:

$$x_k = \begin{bmatrix} p_k \\ v_k \\ \theta_k \end{bmatrix} \tag{2}$$

where p_k, v_k and θ_k denote position, velocity, and attitude angles (roll, pitch, and yaw), respectively.

The system dynamic model can be expressed as:

$$x_k = f(x_{k-1}, u_k) + w_k \tag{3}$$

where u_k represents the control input derived from IMU measurements (acceleration and angular velocity), and w_k denotes process noise.

The discrete-time form is given by:

$$\begin{cases} p_k = p_{k-1} + v_{k-1}\Delta t \\ v_k = v_{k-1} + a_k \Delta t \\ \theta_k = \theta_{k-1} + \omega_k \Delta t \end{cases} \tag{4}$$

The DMI provides displacement observations along the rail direction, with the observation model defined as:

$$z_k = h(x_k) + v_k \tag{5}$$

where z_k is the measured displacement, and v_k represents observation noise.

GNSS provides absolute positioning information in open environments, effectively suppressing long-term drift of the IMU. In GNSS-denied environments, such as tunnels, the system relies on IMU and DMI to maintain short-term stable localization. The EKF is employed to recursively estimate the system state by fusing multi-sensor observations, resulting in high-precision POS, as shown in Figure5. Meanwhile, a dedicated synchronization control circuit is used to ensure unified triggering and precise time alignment among sensors, guaranteeing strict correspondence between point cloud data and pose information.

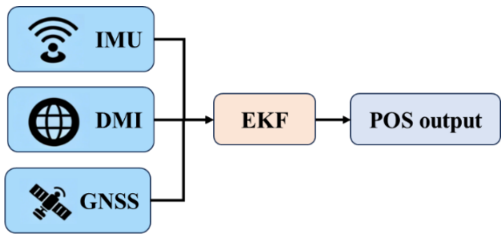

Figure 5: Multi-sensor fusion localization and data flow diagram.

3.2 Point cloud registration and continuous reconstruction

During mobile measurement, point clouds acquired at different time instances are defined in different coordinate systems. Meanwhile, spatial discrepancies (extrinsic parameters) also exist among multiple sensors. Therefore, it is necessary to establish a unified coordinate framework to achieve spatial consistency of multi-source point clouds. Three coordinate systems are defined as world coordinate system of global reference frame (W), body coordinate system of measurement platform (B), and the sensor coordinate system of laser sensor (S), as shown in Figure 6.

The coordinate transformation relationship is expressed as:

$$P_{\mathrm{W}} = T_{\mathrm{WB}} \cdot T_{\mathrm{BS}} \cdot P_{\mathrm{S}} \tag{6}$$

where T_{WB} is the transformation matrix from the body frame to the world frame (provided by the POS), and T_{BS} is the sensor extrinsic calibration matrix.

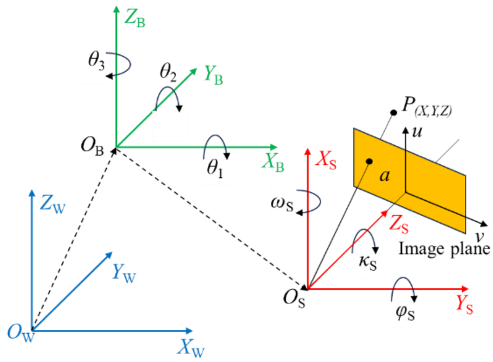

Figure 6: Definition of coordinate systems and transformation relationships.

After obtaining the system pose, local point clouds acquired by the laser scanner are transformed into the global coordinate system. Subsequently, point cloud registration and stitching are performed to achieve continuous rail profile reconstruction.

For each frame, the local point cloud acquired by the laser scanner is defined as:

$$P_{\mathrm{local}}^{k} = \{(x_i, y_i, z_i)\}, i = 1, 2, \ldots, n \tag{7}$$

By fusing IMU and DMI data, the system pose at time step (k) is estimated as:

$$T_k = \begin{bmatrix} R_k & t_k \\ 0 & 1 \end{bmatrix} \tag{8}$$

where R_k is the rotation matrix derived from IMU measurements, and t_k is the translation vector obtained by DMI integration.

The transformation to the global coordinate system is then given by:

$$P_{\mathrm{global}}^{k} = R_k \cdot P_{\mathrm{local}}^{k} + t_k \tag{9}$$

After transforming point clouds into a unified coordinate system, residual errors caused by sensor noise and fusion inaccuracies still lead to spatial misalignment between point clouds acquired at different times and viewpoints. Therefore, further point cloud registration is required.

For each rail, two light sensors are arranged in opposite directions, producing overlapping regions at the rail head. These overlapping regions serve as natural constraints for point cloud registration. Based on this, an improved ICP algorithm is adopted for fine registration. The objective function is defined as:

$$\min_{R,T} \sum_{i=1}^{N} \left\| P_i - (RQ_i + T) \right\|^2 \tag{10}$$

where P_i represents points in the target point cloud, and Q_i represents points in the source point cloud.

As the system moves forward, multi-frame point clouds are continuously accumulated to construct a complete rail profile:

$$P_{\text{global}} = \bigcup_{k=1}^{N} kP_{\text{global}}^{k} \tag{11}$$

To improve both registration accuracy and computational efficiency, several enhancements are introduced, including the initial transformation is provided by IMU-based pose estimation, improving convergence speed and avoiding local minima, the distance between the two rails is constrained to ensure geometric consistency, the key feature points are extracted based on curvature (e.g., rail web region) to enhance registration robustness.

As shown in Figure 7, the coordinate transformation and registration fusion processing flow of rail profile point cloud data is presented. In addition, to improve point cloud quality and achieve accurate continuous profile reconstruction, a systematic processing pipeline is applied to the raw data, including filtering, stitching, and curve fitting. Pass-through filtering and statistical outlier removal are applied to eliminate noise and outliers, followed by Gaussian smoothing to improve data quality. Point clouds are segmented based on mileage information, and local optimization is performed to reduce cumulative errors [18]. Polynomial or spline fitting methods are used to extract key geometric features of the rail cross-section. Multi-frame point clouds are integrated to generate a complete 3D rail model, including the rail head, web, and foot. Finally, by comparing the reconstructed rail profile with the standard rail profile, applications such as rail wear detection, grinding evaluation, and defect identification can be realized.

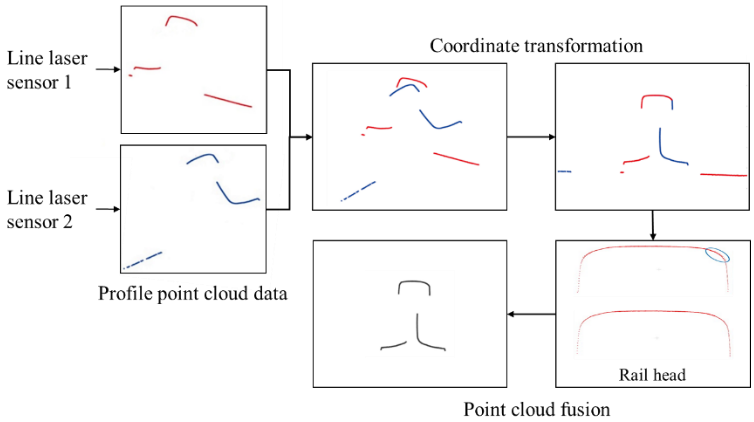

Figure 7: Process of rail profile point cloud coordinate transformation and registration fusion.

4. Line Testing and Accuracy Verification

4.1 Experimental overview

To verify the measurement accuracy and overall performance of the constructed rail continuous profile mobile measurement system, selects the existing railway line to conduct line tests. Based on the complex working conditions of the actual railway operating environment, the system is comprehensively tested. The experiment used a rail inspection vehicle equipped with a measurement system for data collection, as shown in Figure 8, which is a field photo of the continuous profile measurement system for the on-board rail. Before the experiment, the sensor parameters are finely adjusted through system static initialization to ensure the accuracy and stability of data collection. During the experiment, the track inspection car runs along the track at a maximum speed of 60 km/h, and the system synchronously scans and measures the rail continuously. At the same time, to establish a reference benchmark for measurement accuracy, a mature contact type MiniProf measuring instrument was used for manual synchronous measurement in the same section.

(a) (b)

Figure 8: System dynamic installation test. (a) Test vehicle platform; (b) On site diagram.

4.2 System static accuracy verification

After the system equipment is built, static testing is first carried out to verify its basic measurement accuracy. Select a 60 kg/m rail as the test object, randomly mark 3 rail sections in the track, and place the mobile measurement system on the track for measurement, as shown in Figure 9(a). At the same time, using the mature contact type MiniProf measuring instrument results as a benchmark, calculate the remaining deviation and evaluate the static measurement accuracy of the system. The alignment method between the test profile and the comparison profile adopts the principle of "inner alignment", which means aligning based on the center point of the rail top and 16 mm below the working edge rail top, covering the working edge of the rail (left rail -20 °~50 °, right rail -50 °~20 °), and considering the complete profile range of -90 °~90 ° as a whole.

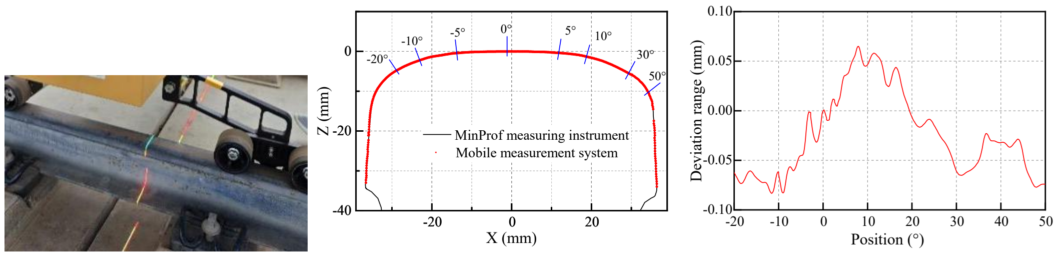

(a) (b) (c)

Figure 9: Static measurement effect of rail profile. (a) System static measurement site; (b) Comparison of profile curves; (c) Remaining static measurement deviation.

Figure 9(b) and 9(c) show the measurement effect of the rail profile at a certain left rail section, including the comparison of profile curves at the rail head and the residual deviation based on profile angles. The results indicate that the point cloud data density on the top surface of the rail is higher than that on the side surface, and the two have the best matching effect on the profile at the top of the rail. At this time, the residual deviation of the working edge of the rail profile is controlled within the range of -0.08 mm to 0.07 mm. Table 1 presents the static measurement results of 5 sections. The results show that the static measurement deviation is basically controlled within the range of ± 0.10 mm, and the optimal accuracy can reach ± 0.06 mm. The measurement results have good repeatability, indicating that the system has high accuracy under static conditions and can meet the requirements of rail profile detection.

Cross-section order	Deviation range (mm)	
	Left	right
1	[-0.08, 0.08]	[-0.09, 0.10]
2	[-0.10, 0.09]	[-0.06, 0.09]
3	[-0.09, 0.09]	[-0.07, 0.09]
4	[-0.08, 0.07]	[-0.10, 0.08]
5	[-0.10, 0.07]	[-0.07, 0.10]

Table 1: Static measurement deviation of rail profile

4.3 System dynamic accuracy verification

On the basis of static accuracy verification, further dynamic testing is carried out to verify the performance of the system under actual mobile measurement conditions. Select an existing railway line for on-site testing, and collect data using a comprehensive inspection train equipped with a measurement system. Considering the initial installation test of the system, in order to increase the longitudinal point cloud density of the rail, the vehicle operating speed is controlled within 60 km/h. Figure 10 shows the actual measured profile of rail cross-section and the continuous 3D point cloud data of the rail profile obtained by the system's mobile measurement. It can be seen that the laser point cloud collected by the system has a high density and can finely present the geometric features of the rail profile.

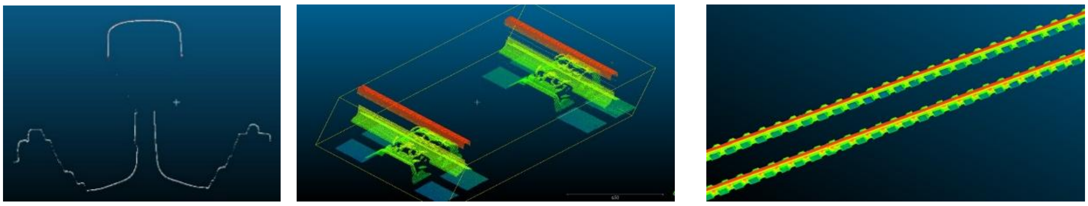

(a) (b) (c)

Figure 10. 3D point cloud model of rail continuous profile. (a) Actual measured profile of rail cross-section; (b) Detailed structure; (c) Partial section.

During the dynamic testing process, three sections were randomly marked on the rail and detection labels were affixed. Through 5 repeated mobile measurement tests, the positioning accuracy of the system was verified using the standard deviation method. Multiple experimental results have shown that the positioning error under dynamic measurement conditions is less than 50 mm, verifying that the system has high positioning accuracy. To further evaluate the dynamic measurement accuracy, the rail profile data at three marked sections were extracted from the three-dimensional point cloud model constructed from five experiments, and compared and analyzed with the contact measurement results of the MiniProf measuring instrument. Table 2 summarizes the residual deviation range of each section and repeated measurement in the dynamic test.

Cross-section order	Repetition number	Deviation range (mm)	
		Left	right
1	1	[-0.09, 0.10]	[-0.08, 0.10]
	2	[-0.09, 0.08]	[-0.08, 0.11]
	3	[-0.09, 0.09]	[-0.06, 0.08]
	4	[-0.09, 0.08]	[-0.08, 0.08]
	5	[-0.09, 0.08]	[-0.06, 0.09]
2	1	[-0.10, 0.10]	[-0.10, 0.10]
	2	[-0.09, 0.08]	[-0.10, 0.15]
	3	[-0.09, 0.10]	[-0.08, 0.10]
	4	[-0.09, 0.08]	[-0.12, 0.11]
	5	[-0.08, 0.09]	[-0.08, 0.07]
3	1	[-0.10, 0.10]	[-0.08, 0.08]
	2	[-0.08, 0.07]	[-0.08, 0.09]
	3	[-0.06, 0.09]	[-0.10, 0.10]
	4	[-0.07, 0.08]	[-0.10, 0.08]
	5	[-0.08, 0.06]	[-0.09, 0.10]

Table 2: Dynamic measurement deviation of rail profile.

The analysis results show that the residual deviation range under dynamic measurement conditions is slightly expanded compared to static measurement, but the vast majority is controlled within the range of -0.10 mm to 0.10 mm, still maintaining high measurement accuracy and meeting the accuracy requirements of actual track measurement. The reason why the dynamic measurement accuracy is slightly lower than the static accuracy is not only affected by human factors, equipment factors, and environmental factors, but also related to the dynamic positioning accuracy of the mobile measurement system in motion.

5. Conclusion

To meet the demand for high-precision and continuous rail profile measurement, a mobile measurement method based on multi-line structured light and integrated navigation is proposed, together with a unified framework combining multi-sensor localization and point cloud reconstruction. The main conclusions are as follows:

(1) A continuous rail profile acquisition method for dynamic scenarios is developed, enabling non-contact and high-density data collection while improving measurement

efficiency and spatial continuity.

(2) A high-precision localization model integrating IMU, DMI, and GNSS is established, cumulative errors of individual sensors are effectively suppressed, providing reliable pose estimation for point cloud reconstruction.

(3) A unified multi-coordinate transformation framework is constructed, and an improved ICP algorithm incorporating initial pose and structural constraints is proposed, significantly enhancing the accuracy and robustness of point cloud registration and enabling continuous 3D reconstruction of rail profiles.

(4) Experimental results demonstrate that the system maintains high accuracy and stability under both static and dynamic conditions, with dynamic measurement deviations generally within ±0.10 mm, meeting engineering requirements.

In summary, the proposed method achieves high accuracy, continuity, and strong engineering applicability, showing great potential for practical deployment in rail condition monitoring and intelligent maintenance. Future work will focus on improving system robustness under high-speed and complex operating conditions and further enhancing multi-source data fusion.

Acknowledgements

This work was supported by National Key Research and Development Program of China (2023YFB2603700), National Natural Science Foundation of China (42501557), China Postdoctoral Science Foundation (2023TQ0253), and State Key Laboratory of Rail Transit Vehicle System Open Project (RVL2505).

References

[1] Q. Zhou, Y. Zhang, F. Liu, et al., "Review of the development of rail technology in high-speed railways", China Railway, (3), 1-8, 2018.

[2] F. Liu, "Tracking study on rail wear of high-speed railway", Railway Engineering, 56(11), 120-123, 2016.

[3] Y. Yang, Q. Xiao, "Influence of personalized rail profile grinding on dynamic performance of EMU", Railway Engineering, 61(10), 120-125, 2021.

[4] EN 15610:2009, "Railway applications-Noise emission-Rail roughness measurement related to rolling noise generation".

[5] D.D. Lichti, "Terrestrial laser scanner self-calibration: Correlation sources and their mitigation", ISPRS Journal of Photogrammetry and Remote Sensing, 61(5), 307-324, 2007.

[6] H. Gonzalez-Jorge, B. Riveiro, P. Arias, et al., "Automatic rail track inspection using laser scanning", Optics and Lasers in Engineering, 51(1), 37-45, 2013.

[7] N. El-Sheimy, H. Hou, X. Niu, "Analysis and modeling of inertial sensors using Allan variance", IEEE Transactions on Instrumentation and Measurement, 57(1), 140-149, 2008.

[8] I. Puente, H. Gonzalez-Jorge, J. Martinez-Sanchez, et al., "Review of mobile

mapping and surveying technologies", Measurement, 46(7), 2127-2145, 2013.
[9] J. Ye, E. Stewart, D. Zhang, et al., "Integration of multiple sensors for non-contact rail profile measurement and inspection", IEEE Transactions on Instrumentation and Measurement, 70, 7002212, 2021.
[10] Z. Liu, J. Sun, H. Wang, et al., "Simple and fast rail wear measurement method based on structured light", Optics and Lasers in Engineering, 49(11), 1343-1351, 2011.
[11] J. Sun, Z. Liu, Y. Zhao, et al., "Motion deviation rectifying method of dynamically measuring rail wear based on multi-line structured-light vision", Optics and Laser Technology, 50, 25-32, 2013.
[12] P. Zhou, K. Xu, D. Wang, "Rail profile measurement based on line-structured light vision", IEEE Access, 6, 16423-16431, 2018.
[13] Y. Shi, Q. Mao, H. Dai, et al., "Research on abnormal vibration of high-speed train based on wheel-rail coupling modal analysis", Vehicle System Dynamics, 1-18, 2024.
[14] Y. Shi, Q. Wang, H. Dai, et al., "Research about carbody abnormal vibration of light rail transit based on suspension failure", Engineering Failure Analysis, 127, 105513, 2021.
[15] Y. Yang, L. Liu, B. Yi, et al., "An accurate and fast method to inspect rail wear based on revised global registration", IEEE Access, 6, 57267-57278, 2018.
[16] K.H. Bae, D.D. Lichti, "Automated registration of unorganised point clouds from terrestrial laser scanners", ISPRS Journal of Photogrammetry and Remote Sensing, 63(1), 36-54, 2008.
[17] P.J. Besl, N.D. McKay, "A method for registration of 3-D shapes", IEEE Transactions on Pattern Analysis and Machine Intelligence, 14(2), 239-256, 1992.
[18] C. Chen, S. Wang, H. Wang, "Accuracy verification method for rail profile measurement system", Railway Engineering, 59(9), 142-145, 2019.